Supplementary Information

Kim, Lara-Gonzalez et al.

I. SUPPLEMENTARY FIGURES & FIGURE LEGENDS

Figure S1, related to figure 1. Localization of the APC/C and monitoring of a Cyclin B::mNeongreen fusion in one-cell *C. elegans* embryos.

Figure S2, related to figure 2. Analysis of the ABBA motif of BUB-1 in control of anaphase onset and in checkpoint signaling.

Figure S3, related to figure 3. Generation of a *cdc-20* deletion mutant, a transgene-based system for CDC-20 replacement with engineered mutants, and analysis of phosphomimetic CDC-20.

Figure S4, related to figure 3. Analysis of CDC-20 N-terminal Cdk phosphorylation sites.

Figure S5, related to figure 4. Analysis of potential kinetochore-localized phosphatases that promote CDC-20 dephosphorylation.

II. SUPPLEMENTARY METHODS, related to Materials & Methods

III. SUPPLEMENTARY TABLES, related to Materials & Methods

Tables S1-S3

IV. SUPPLEMENTARY MOVIE LEGENDS

Movie S1, related to figure 1A

Movie S2, related to figure 1A.

Movie S3, related to figure 1E.

Movie S4, related to figure 2E.

Movie S5, related to figure S2B.

Movie S6, related to figure S2D.

Movie S7, related to figure 2F.

Movie S8, related to figure 3B.

V. SUPPLEMENTARY REFERENCES

I. SUPPLEMENTARY FIGURES & FIGURE LEGENDS

Figure S1. (Related to Figure 1).

Localization of the APC/C and monitoring of a Cyclin B::mNeongreen fusion in one-cell *C. elegans* embryos.

(A) Localization of the essential APC/C subunit Apc1/MAT-2 tagged at its endogenous locus with GFP. No kinetochore localization was detected for the APC/C. Weak chromosomal localization was observed in anaphase. Scale bar, 5 μm.

(B) Images from time-lapse sequences of Cyclin B fused to mNeongreen (CYB-1::mNG). Time above panels is in seconds relative to NEBD. Scale bar, 5 μm.

(C) & (D) Plots of normalized Cyclin B::mNeongreen (mNG) fluorescence for the indicated conditions. Total embryo fluorescence after subtraction of background fluorescence outside the embryo was measured. In *(C)*, the "No Cyclin B::mNG" data points indicate embryo autofluorescence, measured using the same imaging conditions with embryos that express mCherry::H2b but no CYB-1::mNG. The averaged raw intensity values at NEBD without normalization were used to assign the signal intensity at NEBD in the absence versus the presence of CYB-1::mNG signal (there was no significant difference between the raw intensity values at NEBD in the CYB-1::mNG strain for Control and *bub-1(RNAi)*; p=0.31). Subsequent autofluorescence values were plotted relative to the initial assigned intensity. Anaphase onset times are indicated in *(D)*. Data for Control and *bub-1(RNAi)* are the same as in *Fig. 1F*. All error bars are the 95% confidence interval.

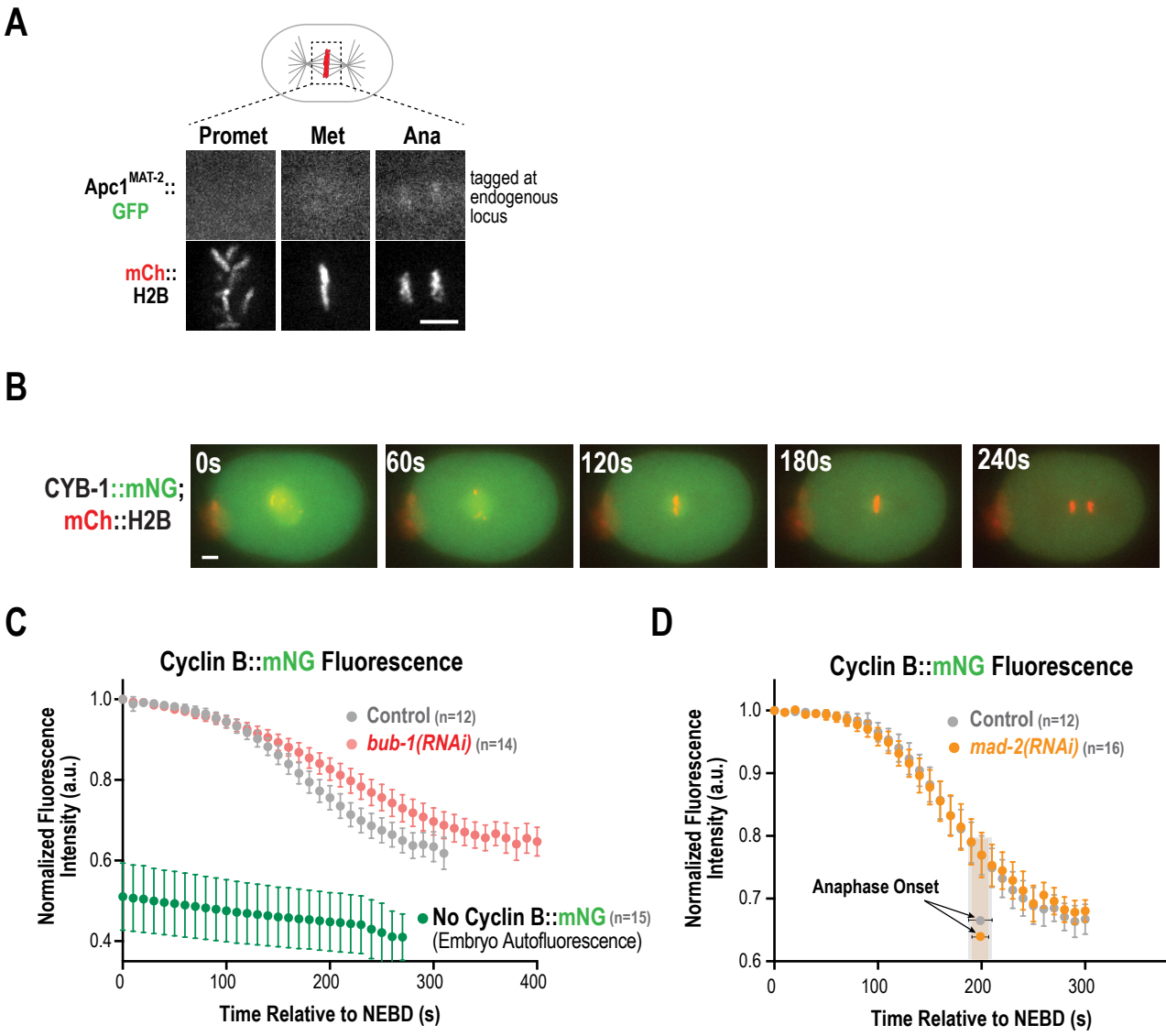
A
Promet
Met
Ana
Apc1MAT-2::GFP
mCh::H2B
tagged at endogenous locus
B
CYB-1::mNG; mCh::H2B
0s
60s
120s
180s
240s
C
Cyclin B::mNG Fluorescence
Normalized Fluorescence Intensity (a.u.)
Control (n=12)
bub-1(RNAi) (n=14)
No Cyclin B::mNG (n=15)
(Embryo Autofluorescence)
Time Relative to NEBD (s)
D
Cyclin B::mNG Fluorescence
Normalized Fluorescence Intensity (a.u.)
Control (n=12)
mad-2(RNAi) (n=16)
Anaphase Onset
Time Relative to NEBD (s)

Figure S2 (related to Figure 2).

Analysis of the ABBA motif of BUB-1 in control of anaphase onset and in checkpoint signaling.

(A) Schematic of BUB-1 and conservation of its ABBA motif in nematode species.

(B) Quantification of NEBD-anaphase onset interval for wildtype versus ABBA mutant BUB-1 in the presence or absence of a temperature-sensitive mutant of Apc8^{MAT-3} (*Apc8^{ts}*). Imaging was performed at the permissive temperature of 22°C, at which the *Apc8^{ts}* mutant is fully viable. p-values are from Mann-Whitney tests.

(C) Schematic summary of sensitized spindle checkpoint assay. Depletion of ZYG-1/Plk4 prevents centriole duplication leading to monopolar spindles in 2-cell embryos. The unattached kinetochores on these monopolar spindles mildly delay mitosis. Creating monopolar spindles in *Apc8^{ts}* at the permissive temperature of 20°C significantly enhances the checkpoint-induced delay, presumably because of an increase in the ratio between unattached kinetochores and their inhibition target, the APC/C (depicted by the red shading in the cartoons) (Bezler and Gonczy 2010).

(D) Images of chromatin morphology on monopolar spindles in the indicated conditions. The frame when decondensation was scored is outlined in green. Times are in seconds after NEBD. Scale bar, 5 μm.

(E) Quantification of mitotic duration, measured as the time from NEBD to chromosome decondensation, in the AB cell of 2-cell embryos for the indicated conditions. *zyg-1(RNAi)* blocks centriole duplication in one-cell embryos and leads to monopolar spindles with unattached kinetochores in 2-cell embryos. *mad-3*Δ removes an essential component of the mitotic checkpoint complex that inhibits the APC/C. Mitotic duration is

greatly increased in the presence of unattached kinetochores in the *Apc8*^{ts} mutant background and this increase is abolished by removal of MAD-3. p-values are from Mann-Whitney tests.

(F) Quantification of checkpoint signaling in 2-cell embryos in the presence of unattached kinetochores for the indicated conditions. Mitotic duration is the NEBD–chromosome decondensation interval in the AB cell. p-values are from Mann-Whitney tests.

(G) Localization of endogenously tagged GFP::MAD-1 at unattached kinetochores on monopolar spindles for the indicated conditions. *zyg-1(RNAi)* was used to create monopolar spindles; the strains assayed also express mCherry::H2b. MAD-1 localization requires BUB-1 but was unaffected by mutation of the ABBA motif in BUB-1. Scale bar 5 μm.

(H) & (I) Embryo viability analysis for the indicated conditions. At least 9 worms and 1087 embryos were scored per condition.

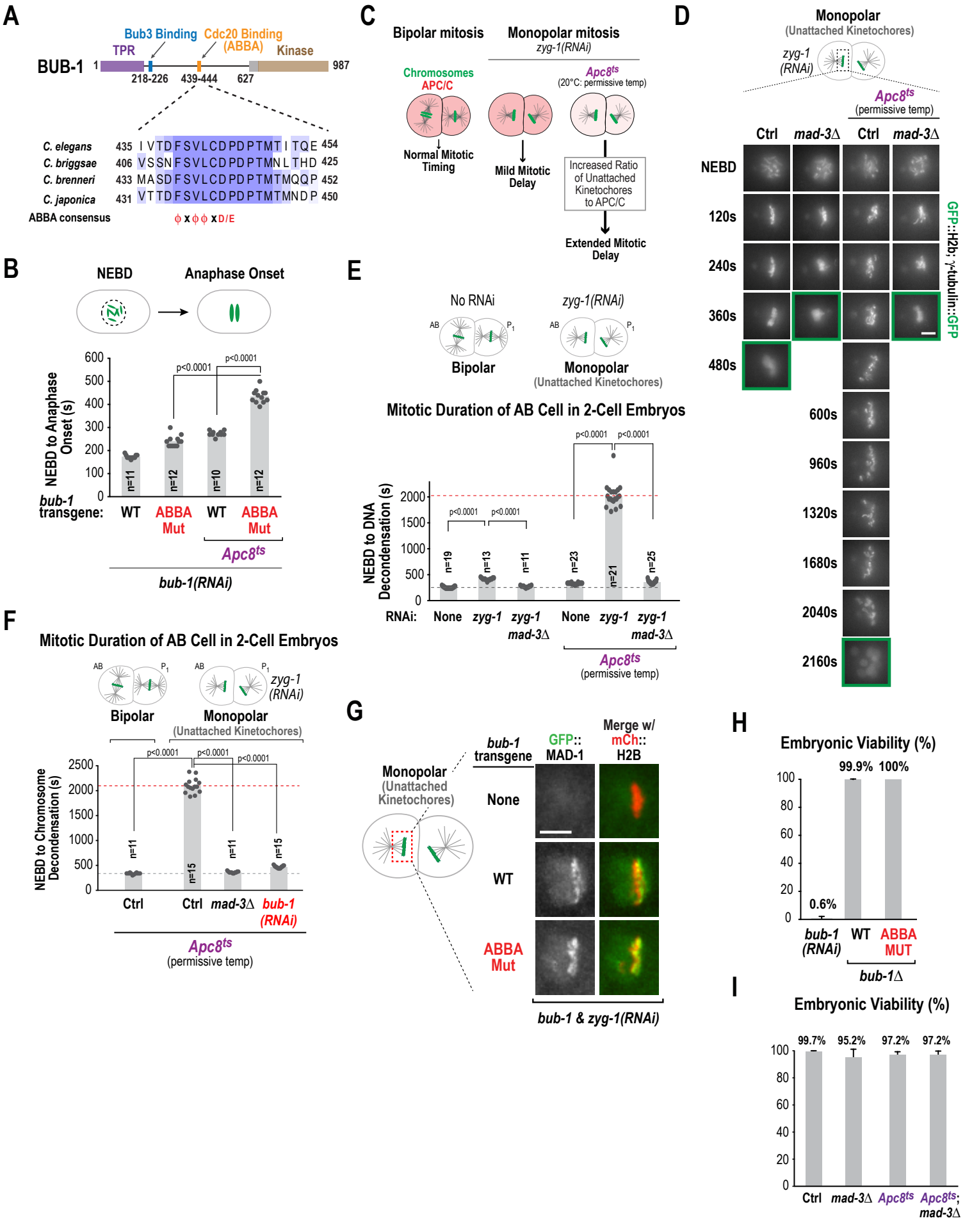
A
Bub3 Binding
Cdc20 Binding (ABBA)
TPR
Kinase
BUB-1
1
987
218-226
439-444
627
C. elegans 435 I V T D F S V L C D P D P T M T I T Q E 454
C. briggsae 406 V S S N F S V L C D P D P T M N L T H D 425
C. brenneri 433 M A S D F S V L C D P D P T M T M Q Q P 452
C. japonica 431 V T T D F S V L C D P D P T M T M N D P 450
ABBA consensus ϕ x ϕ ϕ x D/E
B
NEBD
Anaphase Onset
NEBD to Anaphase Onset (s)
p<0.0001
p<0.0001
n=11
n=12
n=10
n=12
bub-1 transgene:
WT
ABBA Mut
WT
ABBA Mut
Apc8ts
bub-1(RNAi)
C
Bipolar mitosis
Monopolar mitosis
zyg-1(RNAi)
Chromosomes
APC/C
Apc8ts
(20°C: permissive temp)
Normal Mitotic Timing
Mild Mitotic Delay
Increased Ratio of Unattached Kinetochores to APC/C
Extended Mitotic Delay
D
Monopolar
(Unattached Kinetochores)
zyg-1 (RNAi)
Apc8ts
(permissive temp)
Ctrl
mad-3Δ
Ctrl
mad-3Δ
NEBD
120s
240s
360s
480s
600s
960s
1320s
1680s
2040s
2160s
GFP::H2b; γ-tubulin::GFP
E
No RNAi
zyg-1(RNAi)
AB
P1
Bipolar
Monopolar
(Unattached Kinetochores)
Mitotic Duration of AB Cell in 2-Cell Embryos
NEBD to DNA Decondensation (s)
p<0.0001
p<0.0001
p<0.0001
p<0.0001
n=19
n=13
n=11
n=23
n=21
n=25
RNAi:
None
zyg-1
zyg-1 mad-3Δ
None
zyg-1
zyg-1 mad-3Δ
Apc8ts
(permissive temp)
F
Mitotic Duration of AB Cell in 2-Cell Embryos
AB
P1
zyg-1 (RNAi)
Bipolar
Monopolar
(Unattached Kinetochores)
NEBD to Chromosome Decondensation (s)
p<0.0001
p<0.0001
p<0.0001
n=11
n=15
n=11
n=15
Ctrl
Ctrl
mad-3Δ
bub-1 (RNAi)
Apc8ts
(permissive temp)
G
Monopolar
(Unattached Kinetochores)
bub-1 transgene
GFP:: MAD-1
Merge w/ mCh:: H2B
None
WT
ABBA Mut
bub-1 & zyg-1(RNAi)
H
Embryonic Viability (%)
99.9%
100%
0.6%
bub-1 (RNAi)
WT
ABBA MUT
bub-1Δ
I
Embryonic Viability (%)
99.7%
95.2%
97.2%
97.2%
Ctrl
mad-3Δ
Apc8ts
Apc8ts; mad-3Δ

Figure S3 (related to Figure 3).

Generation of a *cdc-20* deletion mutant, a transgene-based system for CDC-20 replacement with engineered mutants, and analysis of phosphomimetic CDC-20.

(A) (*top*) Mos transposon insertion on Chromosome I used to target WT or mutant forms of *cdc-20*, under control of endogenous promoter and UTR sequences. (*bottom*) Details of re-encoding used to alter nucleotide sequence but maintain coding information; a dsRNA to the endogenous sequence of the re-encoded region was employed to deplete endogenous CDC-20 without targeting transgene-encoded CDC-20.

(B) Schematic of the strategy used to generate *cdc-20*Δ, in which CRISPR-Cas9 was used to insert a LoxP site-flanked *Caenorhabditis briggsae unc-119* marker cassette in the *cdc-20* (*fzy-1*) locus, followed by cassette excision using Cre recombinase.

(C) Immunoblot of worm extracts establishing specificity of the CDC-20 antibody. α-tubulin serves as a loading control.

(D) Brood size and embryo viability analysis for the indicated conditions. At least 11 worms and 3000 embryos were scored per condition.

(E) Quantification of NEBD – anaphase onset interval in one-cell embryos in the deletion mutant of *cdc-20*, rescued by WT or 3A transgenes. p-values are from Mann-Whitney tests.

(F) Immunoblot of CDC-20 for the indicated conditions. Note that the 3A and 3D mutants are likely less stable and therefore less expressed. α-tubulin serves as a loading control.

(G) Embryo permeability analysis of phosphomimetic (3D) CDC-20. Defects in APC/C activation perturb meiotic progression and generation of the embryo permeability barrier

that is normally formed prior to anaphase of meiosis II (Olson et al. 2012). A permeability defect results in embryos that exhibit high osmotic sensitivity and limits phenotypic analysis by imaging. Embryo permeability can be monitored by incubation with the lipophilic dye FM4-64. Normal embryos exclude the dye whereas permeable embryos exhibit membrane labeling. The phosphomimetic 3D CDC-20 exhibits a penetrant embryo permeability defect; a similar defect is also observed for the *Apc8*^{ts} mutant at the restrictive temperature (Rappleye et al. 2002).

(H) Embryo viability analysis for the indicated conditions. At least 9 worms and 700 embryos were scored per condition.

Kim, Lara-Gonzalez et al. Figure S3

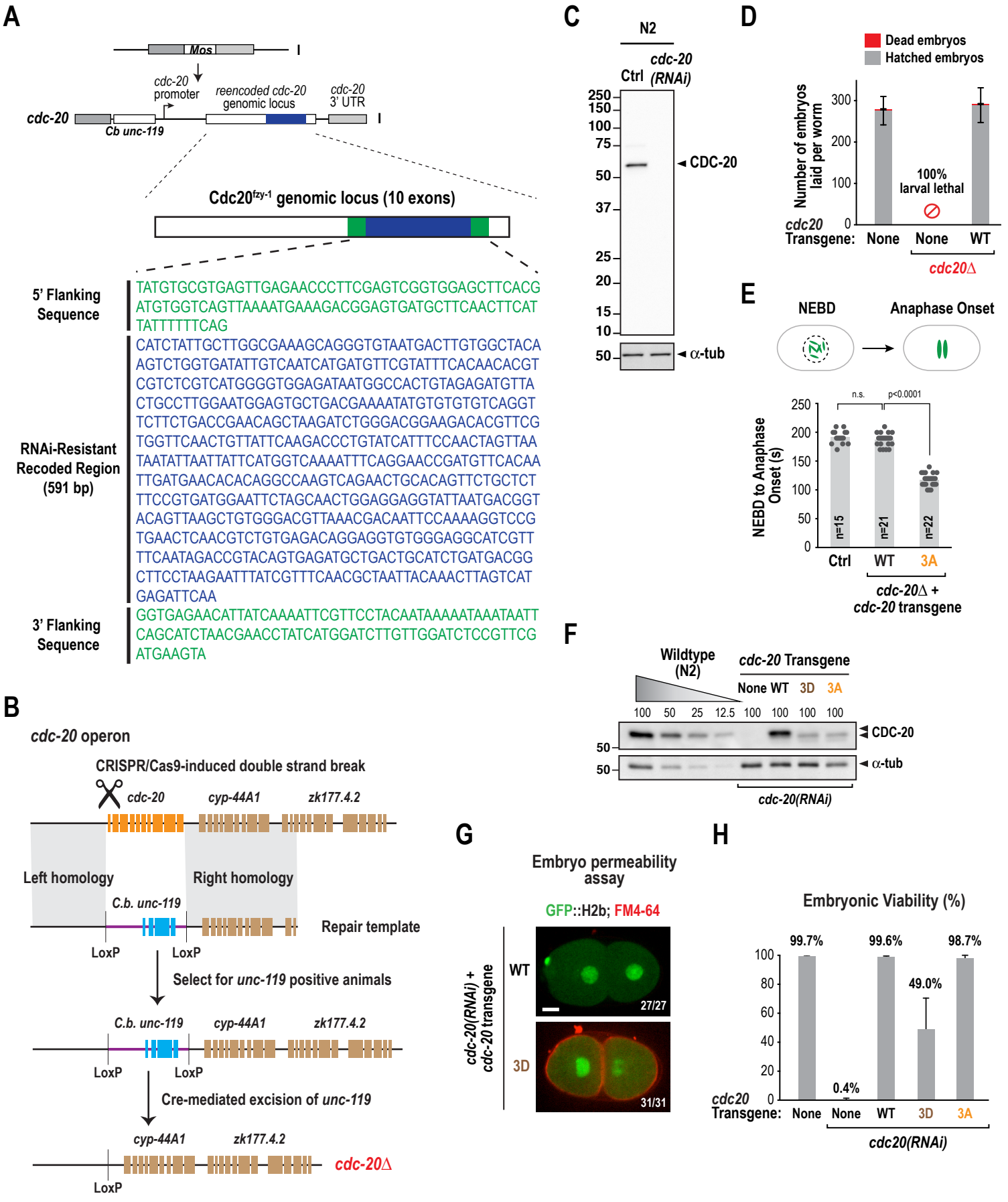

Figure S4 (related to Figure 3).

Analysis of CDC-20 N-terminal Cdk phosphorylation sites.

(A) Quantification of NEBD – anaphase onset interval in one-cell embryos for the indicated conditions. Data for WT and 3A are the same as in *Fig. 3E*. p-values are from Mann-Whitney tests.

(B) Embryo viability analysis for the indicated conditions. At least 12 worms and 780 embryos were scored per condition.

(C) Immunoblot analysis of transgene-encoded CDC-20 (WT, T32A or 3A) in the absence of endogenous CDC-20. α-tubulin serves as a loading control.

(D) Analysis of CDC-20 phospho-isoforms by immunoblotting of a Zinc-Phos-tag gel.

(E) Plot of normalized Cyclin B::mNeongreen (mNG) fluorescence as in *Fig. 1F*.

(F) Analysis of interphase duration, measured as the time from anaphase onset in the 1-cell embryo to NEBD of the AB cell in the 2-cell embryo, for the indicated conditions. Mann-Whitney tests were used to compare the conditions.

(G) Quantification of NEBD to anaphase onset in one-cell embryos following depletion of the sole *C. elegans* Cyclin A (CYA-1). *cya-1(RNAi)* was effective as it resulted in post-embryonic phenotypes, as expected from prior analysis (Rual et al. 2004).

(H) Analysis of spindle checkpoint signaling in the indicated CDC-20 mutants, performed in the *cdc-20*Δ background. The A138V mutant of CDC-20 was previously characterized as being checkpoint-deficient and served as a positive control (Stein et al. 2007; Bezler and Gonczy 2010). p-values are from Mann-Whitney tests.

(I) & (J) Quantification of NEBD – anaphase onset interval in one-cell embryos for the indicated conditions. In (*J)*, data for CDC-20 WT with BUB-1 WT or ABBA are the same as in *Fig. 3H*. p-values are from Mann-Whitney tests.

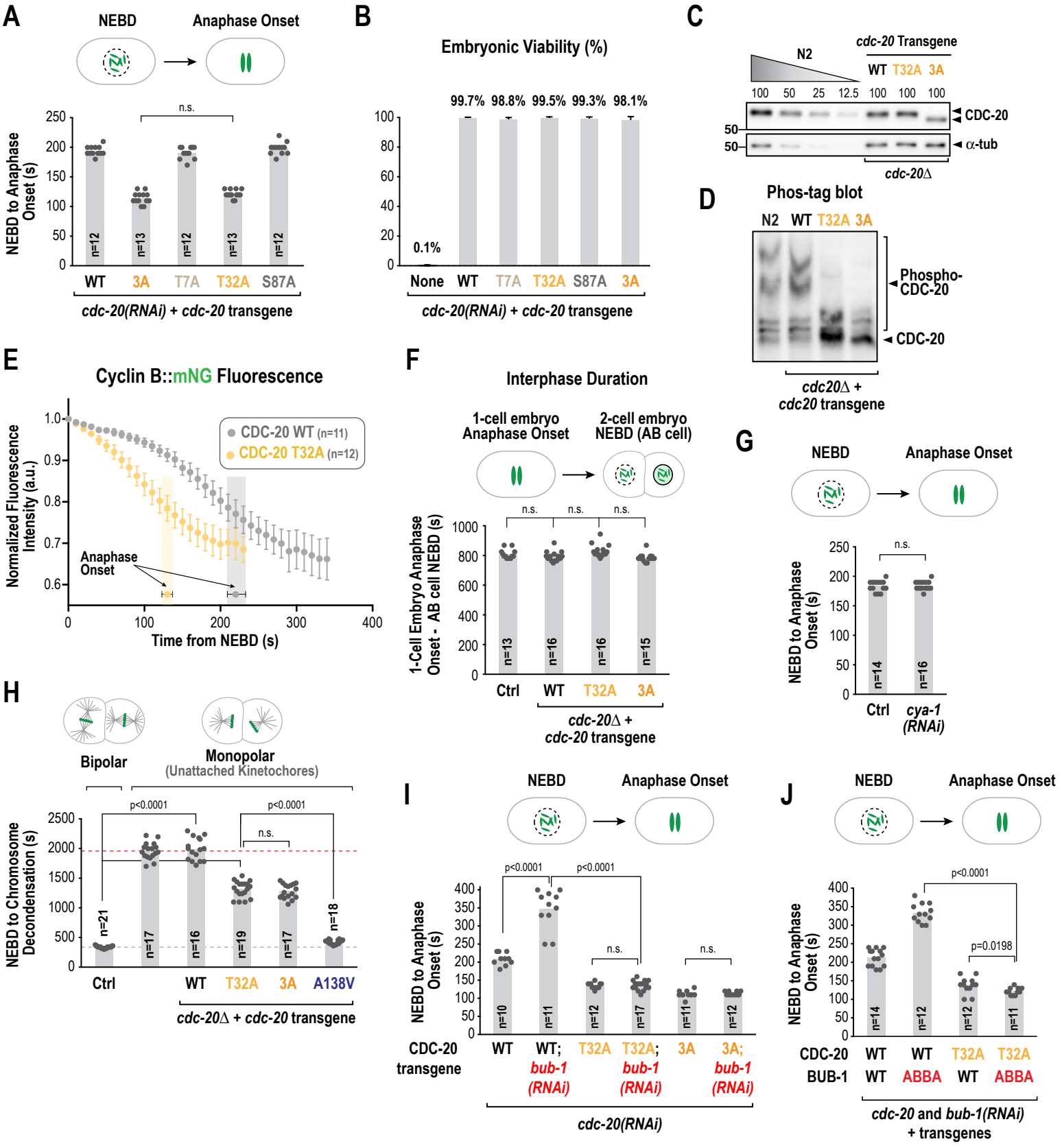
A
NEBD
Anaphase Onset
NEBD to Anaphase Onset (s)
n.s.
n=12
n=13
n=12
n=13
n=12
WT
3A
T7A
T32A
S87A
cdc-20(RNAi) + cdc-20 transgene
B
Embryonic Viability (%)
99.7%
98.8%
99.5%
99.3%
98.1%
0.1%
None
WT
T7A
T32A
S87A
3A
cdc-20(RNAi) + cdc-20 transgene
C
N2
cdc-20 Transgene
WT T32A 3A
100 50 25 12.5 100 100 100
CDC-20
α-tub
cdc-20Δ
D
Phos-tag blot
N2 WT T32A 3A
Phospho-CDC-20
CDC-20
cdc20Δ + cdc20 transgene
E
Cyclin B::mNG Fluorescence
Normalized Fluorescence Intensity (a.u.)
CDC-20 WT (n=11)
CDC-20 T32A (n=12)
Anaphase Onset
Time from NEBD (s)
F
Interphase Duration
1-cell embryo Anaphase Onset
2-cell embryo NEBD (AB cell)
1-Cell Embryo Anaphase Onset - AB cell NEBD (s)
n.s.
n=13
n=16
n=16
n=15
Ctrl
WT
T32A
3A
cdc-20Δ + cdc-20 transgene
G
NEBD
Anaphase Onset
NEBD to Anaphase Onset (s)
n.s.
n=14
n=16
Ctrl
cya-1 (RNAi)
H
Bipolar
Monopolar
(Unattached Kinetochores)
NEBD to Chromosome Decondensation (s)
p<0.0001
p<0.0001
n.s.
n=21
n=17
n=16
n=19
n=17
n=18
Ctrl
WT
T32A
3A
A138V
cdc-20Δ + cdc-20 transgene
I
NEBD
Anaphase Onset
NEBD to Anaphase Onset (s)
p<0.0001
p<0.0001
n.s.
n.s.
n=10
n=11
n=12
n=17
n=11
n=12
CDC-20 transgene
WT
WT; bub-1 (RNAi)
T32A
T32A; bub-1 (RNAi)
3A
3A; bub-1 (RNAi)
cdc-20(RNAi)
J
NEBD
Anaphase Onset
NEBD to Anaphase Onset (s)
p<0.0001
p=0.0198
n=14
n=12
n=12
n=11
CDC-20
WT
WT
T32A
T32A
BUB-1
WT
ABBA
WT
ABBA
cdc-20 and bub-1(RNAi) + transgenes

Figure S5 (related to Figure 4).

Analysis of potential kinetochore-localized phosphatases that promote CDC-20 dephosphorylation.

(A) Images at different mitotic stages of endogenous locus-tagged GSP-1 and GSP-2, the two PP1 catalytic subunits in *C. elegans* embryos (two other catalytic subunits, GSP-3 and GSP-4, are involved in spermatogenesis). GSP-1 shows chromatin and kinetochore localization prior to anaphase. GSP-2 is initially diffuse but shows kinetochore localization just prior to anaphase. Both subunits exhibit robust localization to anaphase chromosomes. Scale bar, 5 μm.

(B) Images from time-lapse sequences of endogenous locus-tagged PPTR-1 and PPTR-2, the two B56 family subunits of PP2A in *C. elegans*. Scale bar, 5 μm.

(C) Embryonic viability analysis for the indicated conditions. At least 9 worms and 740 embryos were scored per condition. The two B56 subunits are redundantly required for viability. Each endogenous locus-tagged B56 subunit rescues the depletion of the other, establishing the functionality of each B56 GFP fusion.

(D) Metaphase stage images from time-lapse sequences of embryos expressing PP1c isoforms (GSP-1 or GSP-2) fused to GFP at their endogenous locus together with transgene-encoded KNL-1::mCherry (WT or $PP1c^{Mut}$); endogenous KNL-1 was depleted. 5 pixel-wide linescans are shown below each image pair. Red curves are KNL-1 normalized to maximal intensity. Green curves are GFP-fused PP1c isoforms normalized to maximal intensity in the presence of KNL-1 WT. Scale bar, 5 μm.

(E) *(top)* Schematics of engineered KNL-1 mutants. PP1c binding and the ability to recruit BUB-1/BUB-3 (by the region containing the 'MELT' repeats (Moyle et al. 2014))

were mutated individually or together. (*bottom*) Quantification of NEBD – anaphase onset interval in one-cell embryos for the indicated conditions. p-values are from Mann-Whitney tests.

(F) Quantification of NEBD – anaphase onset interval in one-cell embryos for the indicated conditions. p-values are from Mann-Whitney tests. Data for CDC-20 WT with KNL-1 WT or PP1c Mut are the same as in *Fig. 4E.*

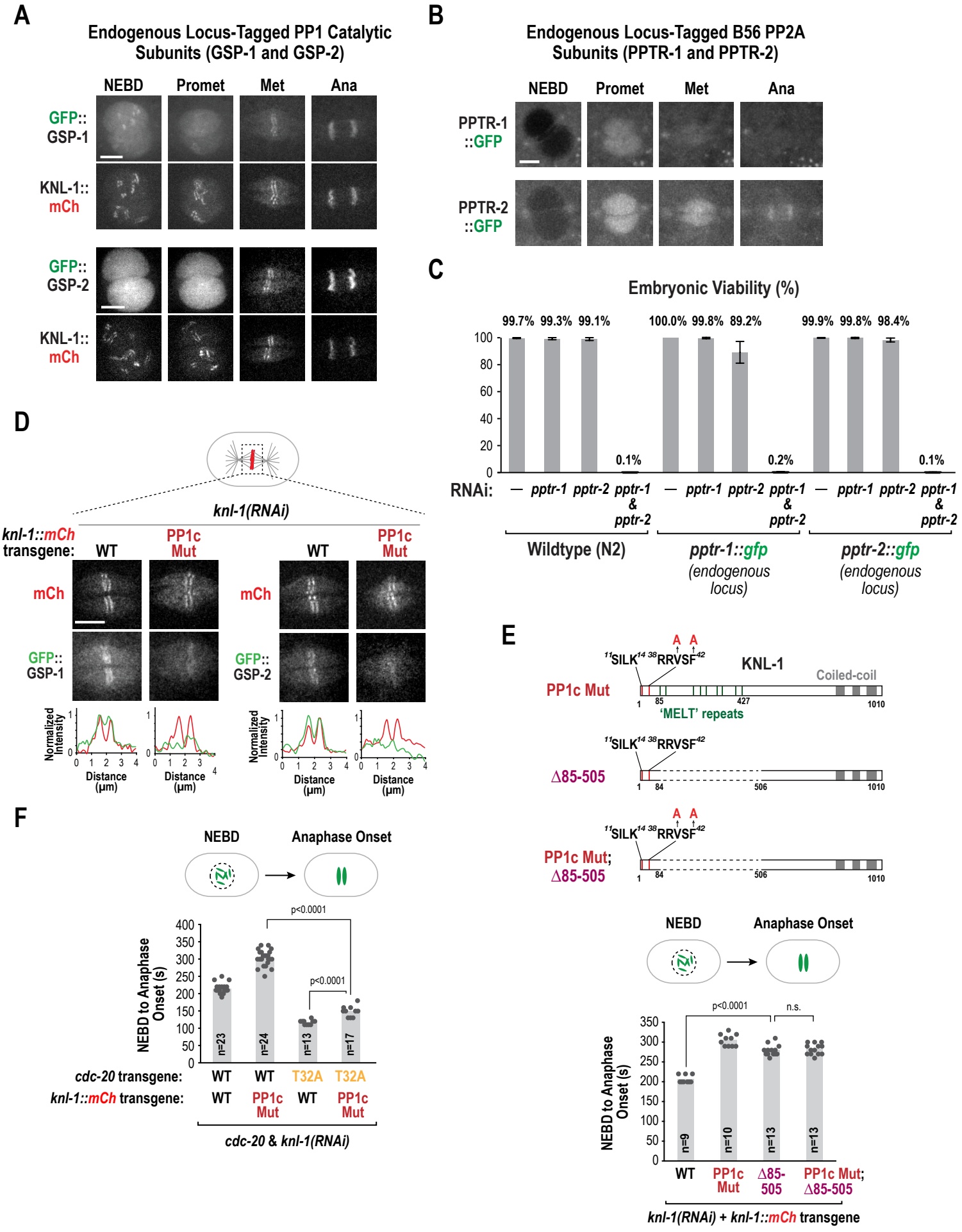
A
Endogenous Locus-Tagged PP1 Catalytic Subunits (GSP-1 and GSP-2)
NEBD
Promet
Met
Ana
GFP:: GSP-1
KNL-1:: mCh
GFP:: GSP-2
KNL-1:: mCh
B
Endogenous Locus-Tagged B56 PP2A Subunits (PPTR-1 and PPTR-2)
NEBD
Promet
Met
Ana
PPTR-1 ::GFP
PPTR-2 ::GFP
C
Embryonic Viability (%)
99.7% 99.3% 99.1% 100.0% 99.8% 89.2% 99.9% 99.8% 98.4%
100
80
60
40
20
0
0.1% 0.2% 0.1%
RNAi: — pptr-1 pptr-2 pptr-1 & pptr-2 — pptr-1 pptr-2 pptr-1 & pptr-2 — pptr-1 pptr-2 pptr-1 & pptr-2
Wildtype (N2)
pptr-1::gfp (endogenous locus)
pptr-2::gfp (endogenous locus)
D
knl-1(RNAi)
knl-1::mCh transgene:
WT
PP1c Mut
WT
PP1c Mut
mCh
GFP:: GSP-1
mCh
GFP:: GSP-2
Normalized Intensity
Distance (µm)
E
11SILK14 38RRVSF42
A A
KNL-1
Coiled-coil
PP1c Mut
1
85
427
1010
'MELT' repeats
Δ85-505
1
84
506
1010
PP1c Mut; Δ85-505
F
NEBD
Anaphase Onset
NEBD to Anaphase Onset (s)
p<0.0001
p<0.0001
n=23
n=24
n=13
n=17
cdc-20 transgene:
knl-1::mCh transgene:
WT
WT
PP1c Mut
WT
T32A
PP1c Mut
cdc-20 & knl-1(RNAi)
NEBD
Anaphase Onset
NEBD to Anaphase Onset (s)
p<0.0001
n.s.
n=9
n=10
n=13
n=13
WT
PP1c Mut
Δ85-505
PP1c Mut; Δ85-505
knl-1(RNAi) + knl-1::mCh transgene

II. SUPPLEMENTARY METHODS, related to Materials & Methods

Generation of single-copy insertion transgenes

RNAi-resistant *bub-1* and *knl-1* transgenes were previously described (Espeut et al. 2012; Moyle et al. 2014; Kim et al. 2015). A *cdc-20* replacement system was generated by PCR-amplification of its genomic locus, which included 2047 bp region upstream of the start codon and 424 bp downstream of the stop codon. For the GFP::CDC-20 transgene, the GFP sequence was inserted after the start codon and was followed by a CPGGGGGGT linker. A segment of *cdc-20* (**Fig. S3A**) was modified to make the transgene RNAi-resistant without altering coding information.

Generation of gene edits by CRISPR/Cas9

The strategy for the generation of the *cdc-20* (*fzy-1*) null allele is described in *Fig. S3B* and it is based on the method described by Dickinson *et al* (Dickinson et al. 2013). Briefly, the strain HT1593 [*unc-119(ed3)III*] was injected with plasmids encoding for Cas9, the *cdc-20* sgRNA (**Table S2**) and a repairing template containing homology arms and C.b.*unc-119* flanked by LoxP sites. Successful integrants, which rescued the *unc-119(ed3)* phenotype, were crossed to the balancer mIn1 and the C.b.*unc-119* cassette was removed by injection of Cre recombinase and selection of organisms that reverted back to the *unc-119(ed3)* mutant phenotype. The resulting *cdc-20*Δ strain was outcrossed against N2 wildtype six times to remove any potential off-target mutations.

To generate endogenous locus-tagged BUB-1::GFP, GFP::GSP-1, PPTR-1::GFP, and PPTR-2::GFP; wildtype N2 worms were injected with plasmids encoding for Cas9, sgRNAs (**Table S2**) and a repairing template containing GFP flanked by 0.8 –

1.0 kb homology arms, along with fluorescent co-injection makers (pGH8, pCFJ90; (Frokjaer-Jensen et al. 2008)) that form extrachromosomal arrays expressing mCherry in the nervous system and pharynx. ~100 mCherry-fluorescent F1 animals were singled to new plates and allowed to lay progeny for 5 days. A subpopulation of worms was collected from each plate, lysed, and analyzed by PCR to identify plates containing GFP integrations. Single progeny from positive plates were allowed to reproduce and analyzed by a new round of PCR to identify homozygous insertions. KNL-1::GFP, tagged at the endogenous locus, was generated using the self-excising cassette method, as described by Dickinson *et al* (Dickinson et al. 2015). Endogenously-tagged GFP::GSP-2 (Hattersley et al. 2016) and GFP::MAD-1 (Wang *et al*, under revision) strains were previously described.

Immunoblotting

For immunoblotting, worm extracts were prepared by lysing gravid adults with 1.5X SDS-sample buffer and sonicating in a water bath at 70^{o}C. The equivalent of 8-10 worms was loaded onto 8% SDS polyacrylamide gels, transferred onto a nitrocellulose membrane and probed with 1 µg/mL of affinity-purified anti-BUB-1 (Oegema et al. 2001), anti-CDC-20 (raised in rabbits against amino acids 1-160 and affinity-purified), or an anti-α-tubulin antibody (DM1α; Sigma-Aldrich) as a loading control..

For Phos-tag gels, Phos-tag (Wako-Chem) was added to polyacrylamide gels at a final concentration of 50 µM, either in the presence of 100 µM $MnCl_2$ (**Fig. 3F**) or 100 µM $ZnCl_2$ (**Fig. S4D**), following the manufacturer's instructions. After electrophoretic running, gels were washed in transfer buffer (48 mM Tris, 39 mM Glycine, 3.5 mM SDS, 20% Methanol) containing 1 mM EDTA for 10 min with agitation, followed by a 10 min wash in

normal transfer buffer. Gels were then transferred to nitrocellulose membranes and probed with anti-CDC-20 antibodies.

Yeast two-hybrid analysis

Yeast-two hybrid assays were performed by cloning cDNAs encoding CDC-20 and BUB-3 into the pGBKT7 vector, and a fragment expressing amino acids 191-472 of BUB-1 (either wild-type or ABBA mutant) into pGADT7. *S. cerevisiae* transformants were plated on –Trp –Leu –His triple dropout plates to test for interactions.

Imaging of *C. elegans* embryos

Time-lapse imaging of strains expressing GFP::H2b and Cyclin B::mNeonGreen; mCherry::H2b was performed on a deconvolution microscope (DeltaVision Elite; Applied Precision) equipped with a charge-coupled device camera (pco.edge 5.5 sCMOS; PCO) and a 60x 1.42NA PlanApo N objective (Olympus). 5x2µm z-stacks without binning were acquired at 10sec intervals. For GFP::H2b, 2% illumination intensity (on an InsightSSI illuminator) and 100 ms exposure was used. For Cyclin B::mNeonGreen;mCherry::H2b, 2% illumination intensity and 300 ms exposure 50% illumination intensity and 100ms exposure for mCh::H2B. All imaging was conducted using an environmental control chamber set at 20°C, unless indicated otherwise.

For all other strains, images were acquired at 20°C on an Andor Revolution XD Confocal System (Andor Technology) with a spinning disk confocal scanner unit (CSU-10; Yokogawa) mounted on an inverted microscope (TE2000-E; Nikon), 100x or 60x 1.4 NA Plan Apochromat lenses, and outfitted with an electron multiplication back-thinned charged-coupled device camera (iXon, Andor Technology). To monitor localization during mitosis, a

5x2 µm z-series without binning was acquired every 20 - 40 sec, with 25 - 100% laser intensity and 50 - 200 ms exposure time for GFP, 100% laser power and 100 - 300 ms exposure time for mCherry.

For FRAP analysis, GFP::CDC-20 and KNL-1::GFP images were acquired in a single z-plane at 0.5 s intervals. Imaging was started ~1 min prior to anaphase onset, as assessed by monitoring chromosome position using mCherry::Histone H2b. After acquisition of the first image, an area of 1.0 x 3.4 µm was photobleached in half of the metaphase plate using an Andor FRAPPA-unit (LC-FPPA-NM10, 405 nm, 0.4 ms pixel dwell time). The high amount of scatter in the *C. elegans* one-cell embryo caused significant photobleaching in the bottom half of the spindle.

Image analysis and quantification

NEBD was defined as the frame where free histone signal in the nucleus equilibrated with the cytoplasm and anaphase onset as the first frame with visible separation of sister chromatids. Cyclin B::mNeonGreen fluorescence was quantified using Image J (Fiji). The integrated intensity of the embryo was measured for each frame; background was measured for an identical-sized region outside the embryo and subtracted from the embryo signal. Imaging of a strain expressing mCh::H2b but not CyclinB::mNeonGreen under identical conditions was used to estimate embryo autofluorescence (*Fig. S1C*). To quantify fluorescence of GFP::CDC-20 and BUB-1::GFP, maximum intensity Z-stack projections were analyzed using Image J (Fiji). A rectangular box was drawn around the metaphase plate and the integrated intensity in the box was recorded. The box was expanded by 5 pixels on each side, and the integrated intensity was measured. The signal and area difference between the expanded box and the original box were used to calculate the

average background signal per pixel. The integrated chromosomal GFP intensity in the original box was then calculated by subtracting the background signal.

For FRAP analysis, fluorescence intensity was quantified as described above, and the GFP::CDC-20 fluorescence intensity curve for the photobleached portion of the plate was fit to a single exponential to determine the fluorescence recovery half time and recovery plateau.

III. SUPPLEMENTARY TABLES

Table S1. *C. elegans* strains used in this study

Strain number	Genotype
N2(ancestral)	
OD56	unc-119(ed3) III; ltIs37[pAA64; pie-1/mCherry::his-58; unc-119 (+)]IV
OD1702	unc-119(ed3)III; ltSi560 [pPLG014; Pmex-5::GFP::his-11::tbb-2_3'UTR, tbg-1::GFP::tbb-2_3'UTR; cb-unc-119(+)]V
OD1095	bub-1(ok3383)I; ltSi268[pOD1951/pTK013; Pbub-1::Bub1 reencoded; cb-unc-119(+)]II; unc-119(ed3)III?
OD1899	san-1(ok1580)I; unc-119(ed3)?III; ltSi560 [pPLG014; Pmex-5::GFP::his-11::tbb-2_3'UTR, tbg-1::gfp::tbb-2_3'UTR; cb-unc-119(+)]V
OD1931	ltSi1[pOD809/pJE110; Pknl-1::knl-1 reencoded::RFP; cb-unc-119(+)]II;unc-119(ed3)III?; ltSi560[pPLG014; Pmex-5::GFP::his-11::tbb-2_3'UTR, GFP::tbg-1::tbb-2_3'UTR; cb-unc-119(+)]V
OD1932	ltSi9[pOD831/pJE120; Pknl-1::knl-1 reencoded(RRASAmutant)::RFP; cb-unc-119(+)]II; unc-119(ed3)III; ltSi560[pPLG014; Pmex-5::GFP::his-11::tbb-2_3'UTR, tbg-1::gfp::tbb-2_3'UTR; cb-unc-119(+)]V
OD1933	ltSi44[pOD1039/pJE170; Pknl-1::knl-1 reencoded(Mutant D85-505)::RFP; cb-unc-119(+)]II; unc-119(ed3)III?; ltSi560[pPLG014; Pmex-5::GFP::his-11::tbb-2_3'UTR, GFP::tbg-1::tbb-2_3'UTR; cb-unc-119(+)]V
OD1934	ltSi585[pPLG022; Pknl-1::knl-1 RRASA(d85-505) reencoded; cb-unc-119(+)]II; unc-119(ed3)III; ltSi560[pPLG014; Pmex-5::GFP::his-11::tbb-2_3'UTR, tbg-1::gfp::tbb-2_3'UTR; cb-unc-119(+)]V
OD2003	unc-119(ed3)? mat-3(or344)III; ltSi560[pPLG014; Pmex-5::GFP::his-11::tbb-2_3'UTR, tbg-1::gfp::tbb-2_3'UTR; cb-unc-119(+)]V
OD2004	san-1(ok1580)I; unc-119(ed3)? mat-3(or344)III; ltSi560 [pPLG014; Pmex-5::GFP::his-11::tbb-2_3'UTR, tbg-1::gfp::tbb-2_3'UTR; cb-unc-119(+)]V
OD2024	ltSi268[pOD1951/pTK013; Pbub-1::Bub1 reencoded; cb-unc-119(+)]II; unc-119(ed3)III?; ltSi560[pPLG014; Pmex-5::GFP::his-11::tbb-2_3'UTR, GFP::tbg-1::tbb-2_3'UTR; cb-unc-119(+)]V
OD2359	fzy-1(lt20::loxP)/mIn1[mIs14 dpy-10(e128)]II
OD2394	ltSi617[pOD1592/pMMB1-1; pbub1::bub1 reencoded exon5/6::bub1 3'UTR; cb-unc-119(+)]I; ltSi9[pOD831/pJE120; Pknl-1::knl-1 reencoded(RRASAmutant)::RFP; cb-unc-119(+)]II; unc-119(ed3)III?; ltSi560 [pPLG014; Pmex-5::GFP::his-11::tbb-2_3'UTR, tbg-1::gfp::tbb-2_3'UTR; cb-unc-119(+)]V
OD2498	ltSi251[pOD1940/pTK002; Pbub-1::GFP-Bub1 reencoded; cb-unc-119(+)]II; unc-119(ed3)III?; ltIs37 [pAA64; pie-1/mCherry::his-58; unc-119(+)]IV
OD2548	ltSi817[pPLG048; Pfzy-1::fzy-1 reencoded::fzy-1 3'UTR; cb-unc-119(+)]I; unc-119(ed3)III
OD2586	ltSi822[pPLG051; Pfzy-1::fzy-1 A138V::fzy-1 3'UTR; cb-unc-119(+)]I; fzy-1(lt20::loxP)II; unc-119(ed3)? mat-3(or344)III; ltSi560[pPLG014; Pmex-5::GFP::his-11::tbb-2_3'UTR, tbg-1::gfp::tbb-2_3'UTR; cb-unc-119(+)]V
OD2591	ltSi814[pPLG047; Pfzy-1::gfp::fzy-1::fzy-1 3'UTR; cb-unc-119(+)]I; unc-119(ed3)III?; ltIs37 [pAA64; pie-1/mCherry::his-58; unc-119 (+)] IV
OD2592	ltSi814[pPLG047; Pfzy-1::gfp::fzy-1::fzy-1 3'UTR; cb-unc-119(+)]I; ltSi268[pOD1951/pTK013; Pbub-1::Bub1 reencoded; cb-unc-119(+)]II; unc-119(ed3)III?; ltIs37 [pAA64; pie-1/mCherry::his-58; unc-119 (+)] IV
OD2664	ltSi805[pPLG042; Pfzy-1::fzy-1::fzy-1 3'UTR; cb-unc-119(+)]I; fzy-1(lt20::loxP)/mIn1[mIs14 dpy-10(e128)]II; unc-119(ed3)?III

OD2692	ltSi805[pPLG042; Pfzy-1::fzy-1::fzy-1 3'UTR; cb-unc-119(+)]I; fzy-1(lt20::loxP)II; unc-119(ed3)?III; ltSi560 [pPLG014; Pmex-5::GFP::his-11::tbb-2_3'UTR, tbg-1::gfp::tbb-2_3'UTR; cb-unc-119(+)]V
OD2693	ltSi805[pPLG042; Pfzy-1::fzy-1::fzy-1 3'UTR; cb-unc-119(+)]I; fzy-1(lt20::loxP)II; unc-119(ed3)? mat-3(or344)III; ltSi560 [pPLG014; Pmex-5::GFP::his-11::tbb-2_3'UTR, tbg-1::gfp::tbb-2_3'UTR; cb-unc-119(+)]V
OD2696	ltSi965[pPLG058; Pfzy-1::fzy-1 T7A, T32A, S87A::fzy-1 3'UTR; cb-unc-119(+)]I; fzy-1(lt20::loxP)/mIn1[mIs14 dpy-10(e128)]II; unc-119(ed3)?III
OD2729	ltSi1112[pOD2673/pTK049; Pcyb-1::cyb-1::mNeongreen::cyb-1 3'UTR; cb-unc-119(+)]I; unc-119(ed3)III?; ltIs37 [pAA64; pie-1/mCherry::his-58; unc-119 (+)] IV
OD2732	ltSi1113[pOD2674/pTK050; Pbub-1::Bub1 reencoded ABBA mut(F440,V442A,L443A,D445A); cb-unc-119(+)]II; unc-119(ed3)III?; ltSi560 [pPLG014; Pmex-5::GFP::his-11::tbb-2_3'UTR, tbg-1::gfp::tbb-2_3'UTR; cb-unc-119(+)]V
OD2737	ltSi814[pPLG047; Pfzy-1::gfp::fzy-1::fzy-1 3'UTR; cb-unc-119(+)]I; ltSi1113[pOD2674/pTK050; Pbub-1::Bub1 reencoded ABBA mut(F440,V442A,L443A,D445A); cb-unc-119(+)]II; unc-119(ed3)III?; ltIs37 [pAA64; pie-1/mCherry::his-58; unc-119 (+)] IV
OD2743	bub-1(ok3383)I;ltSi1113[pOD2674/pTK050; Pbub-1::Bub1 ABBA mut(F440,V442A,L443A,D445A); cb-unc-119(+)]II;unc-119(ed3)III?
OD2798	ltSi268[pOD1951/pTK013; Pbub-1::Bub1 reencoded; cb-unc-119(+)]II; unc-119(ed3)? mat-3(or344)III; ltSi560[pPLG014; Pmex-5::GFP::his-11::tbb-2_3'UTR, GFP::tbg-1::tbb-2_3'UTR; cb-unc-119(+)]V
OD2800	ltSi1113[pOD2674/pTK050; Pbub-1::Bub1 reencoded ABBA mut(F440,V442A,L443A,D445A); cb-unc-119(+)]II; unc-119(ed3)? mat-3(or344) III; ltSi560 [pPLG014; Pmex-5::GFP::his-11::tbb-2_3'UTR, tbg-1::gfp::tbb-2_3'UTR; cb-unc-119(+)]V
OD2896	ltSi1[pOD809/pJE110; Pknl-1::knl-1 reencoded::RFP; cb-unc-119(+)]II; unc-119(ed3)?; gsp-2(lt27[GFP::gsp-2])III
OD2897	ltSi9[pOD831/pJE120; Pknl-1::knl-1 reencoded(RRASAmutant)::RFP; cb-unc-119(+)]II; unc-119(ed3)?; gsp-2(lt27[GFP::gsp-2])III
OD2918	ltSi965[pPLG058; Pfzy-1::fzy-1 T7A, T32A, S87A::fzy-1 3'UTR; cb-unc-119(+)]I; fzy-1(lt20::loxP)II; unc-119(ed3)?III; ltSi560 [pPLG014; Pmex-5::GFP::his-11::tbb-2_3'UTR, tbg-1::gfp::tbb-2_3'UTR; cb-unc-119(+)]V
OD2920	unc-119(ed3)?III; ltIs37[pAA64; pie-1/mCherry::his-58; unc-119 (+)]IV; mdf-1(lt39[gfp::tev::loxP::3xFlag::mdf-1])V
OD2941	ltSi814[pPLG047; Pfzy-1::gfp::fzy-1::fzy-1 3'UTR; cb-unc-119(+)]I; ltSi1[pOD809/pJE110; Pknl-1::knl-1 reencoded::RFP; cb-unc-119(+)]II; unc-119(ed3)III?; ltIs37 [pAA64; pie-1/mCherry::his-58; unc-119 (+)]IV
OD2942	ltSi814[pPLG047; Pfzy-1::gfp::fzy-1::fzy-1 3'UTR; cb-unc-119(+)]I; ltSi9[pOD831/pJE120; Pknl-1::knl-1 reencoded(RRASAmutant)::RFP; cb-unc-119(+)]II; unc-119(ed3)III?; ltIs37 [pAA64; pie-1/mCherry::his-58; unc-119 (+)]IV
OD2944	ltSi1114[pOD2675/pTK051; Pbub-1::Bub1 reencoded ABBA mut(F440,V442A,L443A,D445A); cb-unc-119(+)]I; ltSi9[pOD831/pJE120; Pknl-1::knl-1 reencoded(RRASAmutant)::RFP; cb-unc-119(+)]II; unc-119(ed3)III?; ltSi560 [pPLG014; Pmex-5::GFP::his-11::tbb-2_3'UTR, tbg-1::gfp::tbb-2_3'UTR; cb-unc-119(+)]V
OD2986	ltSi268[pOD1951/pTK013; Pbub-1::Bub1 reencoded; cb-unc-119(+)]II; unc-119(ed3)?III; ltIs37[pAA64; pie-1/mCherry::his-58; unc-119 (+)]IV; mdf-1(lt39[gfp::tev::loxP::3xFlag::mdf-1])V
OD2988	ltSi1113[pOD2674/pTK050; Pbub-1::Bub1 reencoded ABBA mut(F440,V442A,L443A,D445A); cb-unc-119(+)]II; unc-119(ed3)?III; ltIs37[pAA64; pie-1/mCherry::his-58; unc-119 (+)]IV; mdf-1(lt39[gfp::tev::loxP::3xFlag::mdf-1])V
OD3032	ltSi817[pPLG048; Pfzy-1::fzy-1 reencoded::fzy-1 3'UTR; cb-unc-119(+)]I; unc-119(ed3)?III; ltSi560 [pPLG014; Pmex-5::GFP::his-11::tbb-2_3'UTR, tbg-1::gfp::tbb-

	2_3'UTR; cb-unc-119(+)]V
OD3049	ltSi987[pPLG067; Pfzy-1::fzy-1 reencoded T7A, T32A, S87A::fzy-1 3'UTR; cb-unc-119(+)]I; unc-119(ed3)III
OD3050	ltSi987[pPLG067; Pfzy-1::fzy-1 reencoded T7A, T32A, S87A::fzy-1 3'UTR; cb-unc-119(+)]I; unc-119(ed3)?III; ltSi560 [pPLG014; Pmex-5::GFP::his-11::tbb-2_3'UTR, tbg-1::gfp::tbb-2_3'UTR; cb-unc-119(+)]V
OD3075	knl-1(lt53[knl-1::GFP::tev::loxP::3xFlag])III; ltIs37 [pAA64; pie-1/mCherry::his-58; unc-119 (+)] IV
OD3085	ltSi965[pPLG058; Pfzy-1::fzy-1 T7A, T32A, S87A::fzy-1 3'UTR; cb-unc-119(+)]I; fzy-1(lt20::loxP)II; unc-119(ed3)? mat-3(or344)III; ltSi560 [pPLG014; Pmex-5::GFP::his-11::tbb-2_3'UTR, tbg-1::gfp::tbb-2_3'UTR; cb-unc-119(+)]V
OD3086	ltSi1000[pPLG068; Pfzy-1::fzy-1 reencoded T7A::fzy-1 3'UTR; cb-unc-119(+)]I; unc-119(ed3)III
OD3087	ltSi1001[pPLG069; Pfzy-1::fzy-1 reencoded T32A::fzy-1 3'UTR; cb-unc-119(+)]I; unc-119(ed3)III
OD3088	ltSi1002[pPLG070; Pfzy-1::fzy-1 reencoded S87A::fzy-1 3'UTR; cb-unc-119(+)]I; unc-119(ed3)III
OD3089	ltSi1000[pPLG068; Pfzy-1::fzy-1 reencoded T7A::fzy-1 3'UTR; cb-unc-119(+)]I; unc-119(ed3)III; ltSi560 [pPLG014; Pmex-5::GFP::his-11::tbb-2_3'UTR, tbg-1::gfp::tbb-2_3'UTR; cb-unc-119(+)]V
OD3090	ltSi1001[pPLG069; Pfzy-1::fzy-1 reencoded T32A::fzy-1 3'UTR; cb-unc-119(+)]I; unc-119(ed3)III; ltSi560 [pPLG014; Pmex-5::GFP::his-11::tbb-2_3'UTR, tbg-1::gfp::tbb-2_3'UTR; cb-unc-119(+)]V
OD3091	ltSi1002[pPLG070; Pfzy-1::fzy-1 reencoded S87A::fzy-1 3'UTR; cb-unc-119(+)]I; unc-119(ed3)III; ltSi560 [pPLG014; Pmex-5::GFP::his-11::tbb-2_3'UTR, tbg-1::gfp::tbb-2_3'UTR; cb-unc-119(+)]V
OD3110	ltSi817[pPLG048; Pfzy-1::fzy-1 reencoded::fzy-1 3'UTR; cb-unc-119(+)]I; ltSi268[pOD1951/pTK013; Pbub-1::Bub1 reencoded; cb-unc-119(+)]II; unc-119(ed3)III?; ltSi560[pPLG014; Pmex-5::GFP::his-11::tbb-2_3'UTR, GFP::tbg-1::tbb-2_3'UTR; cb-unc-119(+)]V
OD3111	ltSi817[pPLG048; Pfzy-1::fzy-1 reencoded::fzy-1 3'UTR; cb-unc-119(+)]I; ltSi1113[pOD2674/pTK050; Pbub-1::Bub1 reencoded ABBA mut(F440,V442A,L443A,D445A); cb-unc-119(+)]II;unc-119(ed3)III?; ltSi560 [pPLG014; Pmex-5::GFP::his-11::tbb-2_3'UTR, tbg-1::gfp::tbb-2_3'UTR; cb-unc-119(+)]V
OD3112	ltSi965[pPLG058; Pfzy-1::fzy-1 reencoded T7A, T32A, S87A::fzy-1 3'UTR; cb-unc-119(+)]I; ltSi268[pOD1951/pTK013; Pbub-1::Bub1 reencoded; cb-unc-119(+)]II; unc-119(ed3)III?; ltSi560[pPLG014; Pmex-5::GFP::his-11::tbb-2_3'UTR, GFP::tbg-1::tbb-2_3'UTR; cb-unc-119(+)]V
OD3113	ltSi965[pPLG058; Pfzy-1::fzy-1 reencoded T7A, T32A, S87A::fzy-1 3'UTR; cb-unc-119(+)]I; ltSi1113[pOD2674/pTK050; Pbub-1::Bub1 reencoded ABBA mut(F440,V442A,L443A,D445A); cb-unc-119(+)]II; unc-119(ed3)III?; ltSi560 [pPLG014; Pmex-5::GFP::his-11::tbb-2_3'UTR, tbg-1::gfp::tbb-2_3'UTR; cb-unc-119(+)]V
OD3114	ltSi817[pPLG048; Pfzy-1::fzy-1 reencoded::fzy-1 3'UTR; cb-unc-119(+)]I; ltSi1[pOD809/pJE110; Pknl-1::knl-1 reencoded::RFP; cb-unc-119(+)]II; unc-119(ed3)III?; ltSi560 [pPLG014; Pmex-5::GFP::his-11::tbb-2_3'UTR, tbg-1::gfp::tbb-2_3'UTR; cb-unc-119(+)]V
OD3115	ltSi817[pPLG048; Pfzy-1::fzy-1 reencoded::fzy-1 3'UTR; cb-unc-119(+)]I; ltSi9[pOD831/pJE120; Pknl-1::knl-1 reencoded(RRASAmutant)::RFP; cb-unc-119(+)]II; unc-119(ed3)III?; ltSi560 [pPLG014; Pmex-5::GFP::his-11::tbb-2_3'UTR, tbg-1::gfp::tbb-2_3'UTR; cb-unc-119(+)]V
OD3116	ltSi965[pPLG058; Pfzy-1::fzy-1 reencoded T7A, T32A, S87A::fzy-1 3'UTR; cb-unc-119(+)]I; ltSi1[pOD809/pJE110; Pknl-1::knl-1 reencoded::RFP; cb-unc-119(+)]II; unc-119(ed3)III?; ltSi560 [pPLG014; Pmex-5::GFP::his-11::tbb-2_3'UTR, tbg-1::gfp::tbb-2_3'UTR; cb-unc-119(+)]V

OD3117	ltSi965[pPLG058; Pfzy-1::fzy-1 reencoded T7A, T32A, S87A::fzy-1 3'UTR; cb-unc-119(+)]I;ltSi9[pOD831/pJE120; Pknl-1::knl-1 reencoded (RRASAmutant)::RFP; cb-unc-119(+)]II; unc-119(ed3)III?;ltSi560 [pPLG014; Pmex-5::GFP::his-11::tbb-2_3'UTR, tbg-1::gfp::tbb-2_3'UTR; cb-unc-119(+)]V
OD3204	ltSi1001[pPLG069; Pfzy-1::fzy-1 reencoded T32A::fzy-1 3'UTR; cb-unc-119(+)]I; ltSi268[pOD1951/pTK013; Pbub-1::Bub1 reencoded; cb-unc-119(+)]II; unc-119(ed3)III?; ltSi560[pPLG014; Pmex-5::GFP::his-11::tbb-2_3'UTR, GFP::tbg-1::tbb-2_3'UTR; cb-unc-119(+)]V
OD3205	ltSi1001[pPLG069; Pfzy-1::fzy-1 reencoded T32A::fzy-1 3'UTR; cb-unc-119(+)]I; ltSi1113[pOD2674/pTK050; Pbub-1::Bub1 ABBA mut(F440,V442A,L443A,D445A); cb-unc-119(+)]II; unc-119(ed3)III?; ltSi560 [pPLG014; Pmex-5::GFP::his-11::tbb-2_3'UTR, tbg-1::gfp::tbb-2_3'UTR; cb-unc-119(+)]V
OD3206	ltSi1001[pPLG069; Pfzy-1::fzy-1 reencoded T32A::fzy-1 3'UTR; cb-unc-119(+)]I; ltSi1[pOD809/pJE110; Pknl-1::knl-1 reencoded::RFP; cb-unc-119(+)]II; unc-119(ed3)III?; ltSi560 [pPLG014; Pmex-5::GFP::his-11::tbb-2_3'UTR, tbg-1::gfp::tbb-2_3'UTR; cb-unc-119(+)]V
OD3207	ltSi1001[pPLG069; Pfzy-1::fzy-1 reencoded T32A::fzy-1 3'UTR; cb-unc-119(+)]I;ltSi9[pOD831/pJE120; Pknl-1::knl-1 reencoded(RRASAmutant)::RFP; cb-unc-119(+)]II;unc-119(ed3)III?;ltSi560 [pPLG014; Pmex-5::GFP::his-11::tbb-2_3'UTR, tbg-1::gfp::tbb-2_3'UTR; cb-unc-119(+)]V
OD3208	ltSi617[pOD1592/pMMB1-1; pbub1::bub1 reencoded exon5/6::bub1 3'UTR; cb-unc-119(+)]I; ltSi1[pOD809/pJE110; Pknl-1::knl-1 reencoded::RFP; cb-unc-119(+)]II; unc-119(ed3)III?; ltSi560 [pPLG014; Pmex-5::GFP::his-11::tbb-2_3'UTR, tbg-1::gfp::tbb-2_3'UTR; cb-unc-119(+)]V
OD3312	ltSi817[pPLG048; Pfzy-1::fzy-1 reencoded::fzy-1 3'UTR; cb-unc-119(+)]I; ltSi1115[pOD2676/pTK052; Pcyb-1::cyb-1::mNeongreen::cyb-1 3'UTR; cb-unc-119(+)]II; unc-119(ed3)III?; ltIs37[pAA64; pie-1/mCherry::his-58; unc-119 (+)]IV
OD3313	ltSi965[pPLG058; Pfzy-1::fzy-1 reencoded T7A, T32A, S87A::fzy-1 3'UTR; cb-unc-119(+)]I;ltSi1115[pOD2676/pTK052; Pcyb-1::cyb-1::mNeongreen::cyb-1 3'UTR; cb-unc-119(+)]II;unc-119(ed3)III?; ltIs37[pAA64; pie-1/mCherry::his-58; unc-119 (+)]IV
OD3314	ltSi1001[pPLG069; Pfzy-1::fzy-1 reencoded T32A::fzy-1 3'UTR; cb-unc-119(+)]I;ltSi1115[pOD2676/pTK052; Pcyb-1::cyb-1::mNeongreen::cyb-1 3'UTR; cb-unc-119(+)]II;unc-119(ed3)III?; ltIs37[pAA64; pie-1/mCherry::his-58; unc-119 (+)]IV
OD3340	ltSi1058[pPLG149; Pfzy-1::fzy-1 T32A::fzy-1 3'UTR; cb-unc-119(+)]I; fzy-1(lt20::loxP)II; unc-119(ed3)?III
OD3341	ltSi1058[pPLG149; Pfzy-1::fzy-1 T32A::fzy-1 3'UTR; cb-unc-119(+)]I; fzy-1(lt20::loxP)II; unc-119(ed3)?III; ltSi560 [pPLG014; Pmex-5::GFP::his-11::tbb-2_3'UTR, tbg-1::gfp::tbb-2_3'UTR; cb-unc-119(+)]V
OD3342	ltSi1058[pPLG149; Pfzy-1::fzy-1 T32A::fzy-1 3'UTR; cb-unc-119(+)]I; fzy-1(lt20::loxP)II; unc-119(ed3)? mat-3(or344)III; ltSi560 [pPLG014; Pmex-5::GFP::his-11::tbb-2_3'UTR, tbg-1::gfp::tbb-2_3'UTR; cb-unc-119(+)]V
OD3384	ltSi1074[pPLG203; Pfzy-1::fzy-1 T7D, T32D, S87D reencoded::fzy-1 3'UTR; cb-unc-119(+)]I; unc-119(ed3)III
OD3422	ltSi1[pOD809/pJE110; Pknl-1::knl-1 reencoded::RFP; cb-unc-119(+)]II;unc-119(ed3)III?; gsp-1(lt94[gfp::gsp-1])V
OD3423	ltSi9[pOD831/pJE120; Pknl-1::knl-1 reencoded(RRASAmutant)::RFP; cb-unc-119(+)]II; unc-119(ed3)III?; gsp-1(lt94[gfp::gsp-1])V
OD3424	pptr-2(lt91[pptr-2::gfp])V
OD3427	ltSi1074[pPLG203; Pfzy-1::fzy-1 T7D, T32D, S87D reencoded::fzy-1 3'UTR; cb-unc-119(+)]I; unc-119(ed3)III; ltSi560 [pPLG014; Pmex-5::GFP::his-11::tbb-2_3'UTR, tbg-1::gfp::tbb-2_3'UTR; cb-unc-119(+)]V
OD3598	bub-1(lt82[bub-1::gfp])I; ltSi1[pOD809/pJE110; Pknl-1::knl-1 reencoded::RFP; cb-unc-119(+)]II; unc-119(ed3)III?
OD3599	bub-1(lt82[bub-1::gfp])I; ltSi9[pOD831/pJE120; Pknl-1::knl-1 reencoded(RRASAmutant)::RFP; cb-unc-119(+)]II; unc-119(ed3)III?

OD3600	pptr-1(lt89[pptr-1::gfp])V
GAL8	mat-2(mat6[mat-2::GFP::3xFLAG]) II; ltIs37[pie-1p::mCherry::his-58 (pAA64) + unc-119(+)]IV

Table S2. CRISPR sgRNAs used in this study

Target gene no.	Name	Allele generated	gRNA(s) target sequence (5'→3')
ZK177.6	*cdc-20*	*cdc-20*Δ	GGACGCACGCCCGGTAGTGC
W08G11.4	*pptr-1*	*pptr-1::gfp*	GCATTGAAATCGCAATTGTT ACGAGAGAGTGTGTATAAGA
C13G3.3	*pptr-2*	*pptr-2::gfp*	TCTTCTGCATCACTGTTCGT
F29F11.6	*gsp-1*	*gfp::gsp-1*	AAAGTGACCAACAGAAGCCG
C02F5.1	*knl-1*	*knl-1::gfp*	TCGAATGCTGGTGTTCTCTA
R06C7.8	*bub-1*	*bub-1::gfp*	TTGGTTGGCGGCAAGATCAC TCATTGTGTTGGGCTACTTT

Table S3. Oligonucleotides and templates used for dsRNA production

Gene no.	Name	Oligonucleotide (5'→3') #1	Oligonucleotide (5'→3') #2	Template	Conc. (mg/ml)
C02F5.1	*knl-1*	AATTAACCCTCACTAAAGGAATCTCGAATCACCGAAATGTC	TAATACGACTCACTATAGGTTCACAAACTTGGAAGCCGCTG	Genomic DNA	1.2
F59E12.2	*zyg-1*	AATTAACCCTCACTAAAGGTGGACGGAAATTCAAACGAT	TAATACGACTCACTATAGGAACGAAATTCCCTTGAGCTG	cDNA	1.5
Y69A2AR.30	*mad-2*	TAATACGACTCACTATAGGGAGACCACACGGATGTAAAGACACAAAACG	TAATACGACTCACTATAGGGAGACCACGTGAACTGACGTCGAGAATGAG	cDNA	1.8
R06C7.8	*bub-1*	AATTAACCCTCACTAAAGGCCTCATTGAACTTGGAAACC	AATACGACTCACTATAGGGATCCGAATTGGCACATAA	Genomic DNA	3.8
ZK177.6	*cdc-20*	TAATACGACTCACTATAGGCAGCTTCAATTGCATGGAGA	AATTAACCCTCACTAAAGGTGTTCTCACCTTGAATTTCGTG	Genomic DNA	1.2
ZC328.4	*mad-3*	TAATACGACTCACTATAGGCGAAGAACTTCAAAACCTGGA	AATTAACCCTCACTAAAGGTTTGTCGGTCCAGATCCTTC	Genomic DNA	1.5
W08G11.4	*pptr-1*	AATTAACCCTCACTAAAGGCCTCATTGAGGCGACAGCTAATCAATTTGT	TAATACGACTCACTATAGGGATCCGAATTTCGGTTTGTGCAATGGTAG	Genomic DNA	2.2
C13G3.3	*pptr-2*	AATTAACCCTCACTAAAGGCCTCATTGAGTCTACGAGTTTTTCCTGAGAT	TAATACGACTCACTATAGGGATCCGAACATGAACATCTTGAGGGCGTT	Genomic DNA	1.9
ZC328.4	*cya-1*	AATTAACCCTCACTAAAGGTGACGACGATTGTGATGTGAG	TAATACGACTCACTATAGGGGCGGAAAGATTTCCTCGTA	Genomic DNA	1.8

IV. SUPPLEMENTARY MOVIE LEGENDS

Movie S1

Spindle region of *C. elegans* one-cell embryos expressing GFP::CDC-20 and mCherry::H2b (which labels chromatin), filmed through mitosis at 20^{o}C. Time stamp indicates time elapsed after NEBD in seconds. 5 x 2 µm z-stacks were acquired every 20 seconds and maximal intensity projections generated for each time frame. Playback rate is 6 frames per second, or 120X relative to real time. *Related to Fig. 1A*.

Movie S2

Spindle region of *C. elegans* one-cell embryos expressing GFP::BUB-1 and mCherry::H2b (which labels chromatin), filmed through mitosis at 20^{o}C. Time stamp indicates time elapsed after NEBD in seconds. 5 x 2 µm z-stacks were acquired every 20 seconds and maximal intensity projections generated for each time frame. Playback rate is 6 frames per second, or 120X relative to real time. *Related to Fig. 1A*.

Movie S3

Spindle region of *C. elegans* one-cell embryos depleted of endogenous BUB-1 by RNAi, expressing the *Apc8^{ts}* mutant, or the combination of the two. Embryos expressed GFP::H2b and γ-tubulin::GFP, which mark the chromosomes and spindle poles, respectively, and were filmed through mitosis at the permissive temperature of 22^{o}C. Time stamp indicates time elapsed after NEBD in seconds. 5 x 2 µm z-stacks were acquired every 10 seconds and maximal intensity projections were generated for each time frame. Playback rate is 6 frames per second, or 60X relative to real time. *Related to Fig. 1E*.

Movie S4

Spindle region of *C. elegans* one-cell embryos depleted of endogenous BUB-1 by RNAi and expressing the indicated transgene-encoded BUB-1 versions. Embryos expressed GFP::H2b and γ-tubulin::GFP, which mark the chromosomes and spindle poles, respectively, and were filmed through mitosis at 20°C. Time stamp indicates time elapsed after NEBD in seconds. 5 x 2 µm z-stacks were acquired every 10 seconds and maximal intensity projections generated for each time frame. Playback rate is 6 frames per second, or 60X relative to real time. *Related to Fig. 2E*.

Movie S5

Spindle region of *C. elegans* one-cell embryos depleted of endogenous BUB-1 by RNAi and expressing the indicated transgene-encoded BUB-1 versions, either in the presence of absence of the *Apc8*^{ts} allele. Embryos expressed GFP::H2b and γ-tubulin::GFP, which mark the chromosomes and spindle poles, respectively, and were filmed through mitosis at the permissive temperature of 22^{o}C. Time stamp indicates time elapsed after NEBD in seconds. 5 x 2 µm z-stacks were acquired every 10 seconds and maximal intensity projections generated for each time frame. Playback rate is 6 frames per second, or 60X relative to real time. *Related to Fig. S2B*.

Movie S6

Spindle region of the AB cell of two-cell *C. elegans* embryos, induced to form monopolar spindles by preventing centriole duplication in the zygote using RNAi-mediated depletion of ZYG-1/Plk4. Monopolar spindles were imaged in the presence of the *Apc8*^{ts} allele, the *mad-3*Δ allele or the *Apc8*^{ts};*mad-3*Δ double mutant. Embryos expressed GFP::H2b and γ-tubulin::GFP, which mark the chromosomes and spindle poles, respectively, and were filmed through mitosis at the permissive temperature of 20^{o}C. Time stamp indicates time elapsed after NEBD in

seconds. 5 x 2 μm z-stacks were acquired every 20 seconds and maximal intensity projections generated for each time frame. Playback rate is 6 frames per second, or 120X relative to real time. *Related to Fig. S2D*.

Movie S7

Spindle region of the AB cell of two-cell *Apc8^{ts} C. elegans* embryos, induced to form monopolar spindles by preventing centriole duplication in the zygote using RNAi-mediated depletion of ZYG-1/Plk4. Where indicated, embryos were co-depleted of BUB-1 in the presence or absence of the indicated transgene-encoded BUB-1 versions. Embryos expressed GFP::H2b and γ-tubulin::GFP, which mark the chromosomes and spindle poles, respectively, and were filmed through mitosis at 20^{o}C. Time stamp indicates time elapsed after NEBD in seconds. 5 x 2 μm z-stacks were acquired every 20 seconds and maximal intensity projections generated for each time frame. Playback rate is 6 frames per second, or 120X relative to real time. *Related to Fig. 2F*.

Movie S8

Spindle region of one-cell *C. elegans* embryos depleted of endogenous CDC-20 by RNAi and expressing the indicated transgene-encoded CDC-20 versions. Embryos expressed GFP::H2b and γ-tubulin::GFP, which mark the chromosomes and spindle poles, respectively, and were filmed through mitosis at 20^{o}C. Time stamp indicates time elapsed after NEBD in seconds. 5 x 2 μm z-stacks were acquired every 10 seconds and maximal intensity projections generated for each time frame. Playback rate is 6 frames per second, or 60X relative to real time. *Related to Fig. 3B*.

V. SUPPLEMENTARY REFERENCES

Bezler A, Gonczy P. 2010. Mutual antagonism between the anaphase promoting complex and the spindle assembly checkpoint contributes to mitotic timing in Caenorhabditis elegans. *Genetics* **186**: 1271-1283.

Dickinson DJ, Pani AM, Heppert JK, Higgins CD, Goldstein B. 2015. Streamlined Genome Engineering with a Self-Excising Drug Selection Cassette. *Genetics* **200**: 1035-1049.

Dickinson DJ, Ward JD, Reiner DJ, Goldstein B. 2013. Engineering the Caenorhabditis elegans genome using Cas9-triggered homologous recombination. *Nat Methods* **10**: 1028-1034.

Espeut J, Cheerambathur DK, Krenning L, Oegema K, Desai A. 2012. Microtubule binding by KNL-1 contributes to spindle checkpoint silencing at the kinetochore. *J Cell Biol* **196**: 469-482.

Frokjaer-Jensen C, Davis MW, Hopkins CE, Newman BJ, Thummel JM, Olesen SP, Grunnet M, Jorgensen EM. 2008. Single-copy insertion of transgenes in Caenorhabditis elegans. *Nat Genet* **40**: 1375-1383.

Hattersley N, Cheerambathur D, Moyle M, Stefanutti M, Richardson A, Lee KY, Dumont J, Oegema K, Desai A. 2016. A Nucleoporin Docks Protein Phosphatase 1 to Direct Meiotic Chromosome Segregation and Nuclear Assembly. *Dev Cell* **38**: 463-477.

Kim T, Moyle MW, Lara-Gonzalez P, De Groot C, Oegema K, Desai A. 2015. Kinetochore-localized BUB-1/BUB-3 complex promotes anaphase onset in C. elegans. *J Cell Biol* **209**: 507-517.

Moyle MW, Kim T, Hattersley N, Espeut J, Cheerambathur DK, Oegema K, Desai A. 2014. A Bub1-Mad1 interaction targets the Mad1-Mad2 complex to unattached kinetochores to initiate the spindle checkpoint. *J Cell Biol* **204**: 647-657.

Oegema K, Desai A, Rybina S, Kirkham M, Hyman AA. 2001. Functional analysis of kinetochore assembly in Caenorhabditis elegans. *J Cell Biol* **153**: 1209-1226.

Olson SK, Greenan G, Desai A, Muller-Reichert T, Oegema K. 2012. Hierarchical assembly of the eggshell and permeability barrier in C. elegans. *J Cell Biol* **198**: 731-748.

Rappleye CA, Tagawa A, Lyczak R, Bowerman B, Aroian RV. 2002. The anaphase-promoting complex and separin are required for embryonic anterior-posterior axis formation. *Dev Cell* **2**: 195-206.

Rual JF, Ceron J, Koreth J, Hao T, Nicot AS, Hirozane-Kishikawa T, Vandenhaute J, Orkin SH, Hill DE, van den Heuvel S et al. 2004. Toward improving Caenorhabditis elegans phenome mapping with an ORFeome-based RNAi library. *Genome Res* **14**: 2162-2168.

Stein KK, Davis ES, Hays T, Golden A. 2007. Components of the spindle assembly checkpoint regulate the anaphase-promoting complex during meiosis in Caenorhabditis elegans. *Genetics* **175**: 107-123.